



Effect of reduction potential and post-deposition annealing on the structural, compositional and optical properties of electrodeposited copper(I) sulfide thin films

R. Torres-Ricárdez¹ · E. Ramírez-Morales¹ · L. Rojas-Blanco¹ · F. I. Lizama-Tzec² · M. F. García-Mendoza¹ · J. G. Álvarez-Ramírez¹ · L. L. Díaz-Flores¹ · G. Pérez-Hernández¹

Received: 16 December 2017 / Accepted: 5 April 2018 / Published online: 9 April 2018
© Springer Science+Business Media, LLC, part of Springer Nature 2018

Abstract

In the present work it is reported on the deposition of cuprous sulfide (Cu_2S) by the electrodeposition technique and its characterization followed by a heat treatment. Cu_2S films were deposited using reduction potentials in a range of -600 to -555 mV (vs. SCE) with a deposition time of 1000 s. The annealing process was performed varying the atmosphere (inert or with sulfur) and temperature (250 and 350 °C). The properties of deposited Cu_2S films were analyzed using UV–Vis spectroscopy, X-ray diffraction, scanning electron microscopy and energy-dispersive X-ray spectroscopy. The deposited films had a hexagonal structure in the chalcocite phase and showed a band gap in the range of 1.61 and 1.8 eV. Characterization techniques demonstrated modifications in the properties of the material due to the presence or deficiency of sulfur in the films.

1 Introduction

Copper sulfide is a semiconductor that is widely used in the conversion of solar energy in solar cells, catalysis, biosensors, optoelectronic applications and field emission devices [1–4]. Due to its low toxicity, low absorption coefficient ($< 10^4 \text{ cm}^{-1}$) and abundance of its constituent elements [5, 6], it has been used in cells sensitized with dyes and as a precursor of the $\text{Cu}_2\text{ZnSnS}_4$ absorber material (CZTS) [7, 8].

The electrodeposition technique is a simple method for the deposition of thin films since it is carried out under ambient conditions or at low temperatures, and consumes the largest amount of reactive material. The electrodeposition process consists of the immersion of a substrate in a solution of metal ions and the application of a potential or current that causes the ions to be reduced at the surface of the substrate [9]. Copper sulfide has different phases, from copper enriched to sulfur enriched, including many known solid

phases, such as covellite (CuS), anilite ($\text{Cu}_{1.75}\text{S}$), digenite ($\text{Cu}_{1.8}\text{S}$), djurleite ($\text{Cu}_{1.96}\text{S}$) and chalcocite (Cu_2S) [10–13], which can be obtained by modifying the applied potential or current. These phases have different physical characteristics; in particular, different values of the band gap, from 1.2 to 2.0 eV [14].

Various synthesis methods of copper sulfide films, both chemical and physical, including spray pyrolysis, chemical vapor deposition, chemical bath deposition, solvothermal and electrochemical methods have been studied [15–20]. However, the effect of the lack of Cu or S in the different phases of Cu_2S is not completely understood, and is necessary to find the best conditions for its various applications. In the present work, the effects of the change of reduction potentials during deposition on the structural, morphological and optical properties of copper sulfide thin films have been studied. To improve the physical properties of the obtained films, they were thermally treated at different temperatures and under different atmospheres.

2 Experimental details

2.1 Materials

Fluorine-doped tin oxide (FTO) was used as conductive glass (TEC 15, resistivity: 12–14 Ωm , transmittance: 82–84.5%,

✉ G. Pérez-Hernández
german.perez@ujat.mx

¹ Universidad Juárez Autónoma de Tabasco, Avenida Universidad S/N, Zona de la Cultura, Col. Magisterial, Centro, 86040 Villahermosa, Tabasco, Mexico

² Departamento de Física Aplicada, CINVESTAV-IPN, 97310 Merida, Yucatán, Mexico

Hartford glass), with dimensions of 10 × 25 mm. A 50 ml solution was prepared by adding 0.1 M NaCl (≥ 99%, Sigma-Aldrich), 4 mM CuSO₄·5H₂O (99%, Sigma-Aldrich), 50 mM sodium thiosulfate (99%, Sigma-Aldrich), 0.25 M Tribasic sodium citrate dihydrate (≥ 99%, Sigma-Aldrich), and the pH modifying agent HCl and/or NaOH.

2.2 Electrochemical techniques

To determine the range of potentials to be used during deposition, cyclic voltammetry was performed using a potentiostat AUTOLAB PGSTAT 128N, a platinum wire as a counter electrode and a saturated calomel electrode (SCE) [21] as the reference electrode between two potential limits (650 to –850 mV). All potentials are shown with reference to SCE. The experiments were carried out at a temperature of 80 °C while maintaining a pH of 4.75.

The deposition process was performed using the chronoamperometry technique, using deposition potentials within the determined range over a period of 1000 s. The heat treatment was carried out in a MTI Corporation GSL-1100X tubular furnace, in both nitrogen and sulfur atmospheres under nitrogen flow (0.05 g of sulfur). All treatments were performed over a period of 1 h.

2.3 Characterization

The obtained thin films were subjected to various characterization techniques to evaluate their structural, morphological and optical properties. The crystal structure of the films was determined by X-ray diffraction (XRD) using a RIGAKU X-ray diffractometer, Smartlab model, in the blending mode with Cu K α radiation source ($\lambda = 1.54056 \text{ \AA}$), and with an angle of incidence of 0.5° in a 2 theta (2θ) range of 20°–90°. In the morphological analysis, a scanning electron microscope (SEM) JEOL JSM-6010LA was used at 10 kV acceleration voltage under high vacuum conditions at 20,000×. A dispersive energy detector (EDX) coupled to the SEM was used to perform the qualitative analysis and distribution of elements on the surface of the samples. The optical properties were analyzed in an Agilent G1103A UV–Vis spectrophotometer in transmittance mode in a wavelength range of 190–1100 nm.

3 Results and discussion

3.1 Electrochemical analysis

Cyclic voltammetry was performed in an aqueous solution containing copper (Cu²⁺) and thiosulfate (S₂O₃²⁻) ions in the presence of the sodium citrate complexing agent (Na₃C₆H₅O₇). Figure 1 shows the cyclic voltammogram of

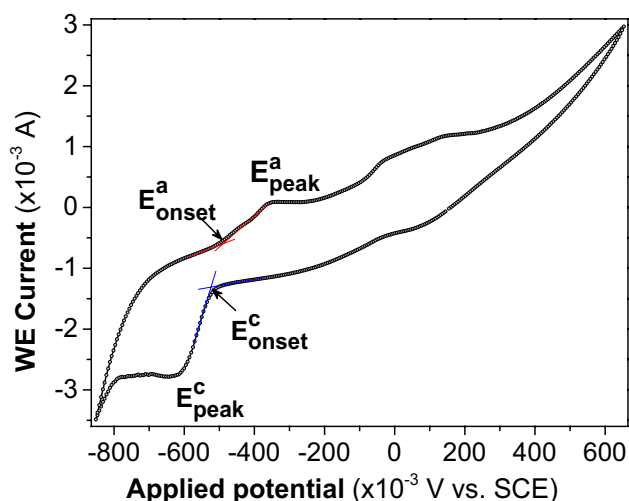
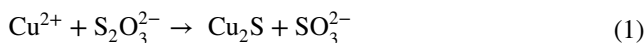


Fig. 1 Cyclic voltammetry of Cu₂S electrochemical solution

the aqueous solution, observing the cathodic peak potential (E_{peak}^c) at –600 mV and the corresponding onset potential (E_{onset}^c) at –520 mV [22]. In addition, the anodic peak potential (E_{peak}^a) was found at –350 mV and the onset potential (E_{onset}^a) at –480 mV, indicating a copper oxidation process. These results can be associated with the Cu²⁺ and S₂O₃²⁻ reduction process, which corresponds to the deposition process at the electrode, according to the following mechanism [23, 24]:

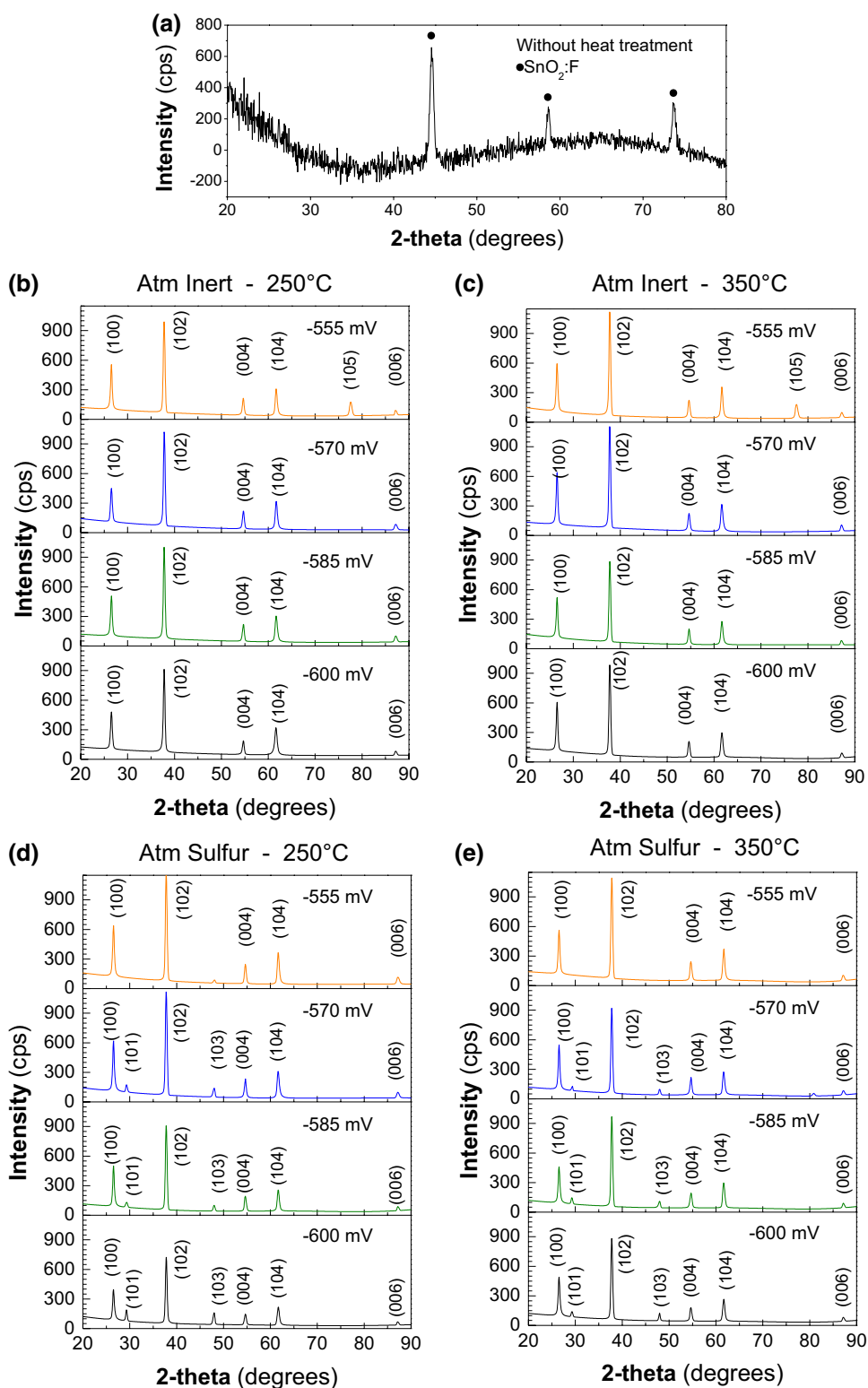


Based on these results, the potential range for film deposition was determined, and four different potentials were established: –600, –585, –570 and –555 mV (all vs. SCE).

3.2 Structural analysis

The XRD patterns of the deposited Cu₂S films are shown in Fig. 2. Figure 2a shows the Cu₂S films XRD spectrum without heat treatment, in which the characteristic reflection peaks of the FTO planes (210), (002) and (212) of SnO₂ can be observed. The Cu₂S characteristic plane is not observed, indicating an amorphous phase condition of the material, requiring post-deposition treatment to achieve crystallinity in the deposited films. This contrasts with that obtained by Giaccherini et al. [25], which states that the electrodeposited films of copper sulfide phases are crystalline, however, this difference is the result of the conditions used in both experiments, such as the applied potentials, the reagents and the electrodes.

Fig. 2 XRD pattern of Cu_2S films treated under conditions of **a** without heat treatment, **b** atm. inert $T=250^\circ\text{C}$, **c** atm. inert $T=350^\circ\text{C}$, **d** atm. sulfur $T=250^\circ\text{C}$, **e** atm. sulfur $T=350^\circ\text{C}$



The films exposed to heat treatment at 250°C in an inert atmosphere, shown in Fig. 2b, have perfectly superimposed patterns for the deposits that range from -600 to -555 mV. The largest intensity peak is observed at 37.8° in the four diffraction patterns, which is characteristic of the plane (102)

of the hexagonal structure in the high chalcocite phase (PDF #01-078-4793). In the films treated under inert atmosphere at 250°C (Fig. 2b) and 350°C (Fig. 2c), it is possible to observe the existence of a peak in the pattern of the deposit prepared at -555 mV, which is related to the FTO substrate

and can be attributed to the smaller thickness of the films. In the diffraction patterns of films treated under a sulfur atmosphere (Fig. 2d, e), there are peaks that are centered around a 2-theta value of 29.16° (101) and 48.10° (103). These peaks are not appreciated in the inert atmosphere treatments, and are characteristic of the hexagonal structure in the high chalcocite phase (PDF # 01-084-0206). These planes are possibly caused by the modification of copper content with respect to sulfur content in the crystalline structure of the films, due to the incorporation of sulfur during the post-deposition treatment, originated from the transformation of the c-axis of the monoclinic Cu₂S into the c-axis of the hexagonal Cu₂S, owing to the positional disorder of the Cu atoms [26]. It is observed that in the films deposited at –555 mV, the diffraction peaks relative to the planes (101) and (103) decrease in intensity or do not occur. This is propitiated by the more negative potentials applied during deposition, and possibly related to dissolution–reprecipitation processes or transformation in the solid phase [27].

The analyzed Cu₂S films do not show a significant change in particle size, with values in the range of 160–180 nm. The particle size was determined using the Scherrer equation from the Bragg reflection width [28].

The lattice parameters of the crystal structure were determined from the XRD diffraction patterns (Fig. 2), finding values for *a* between 3.86 and 3.94 Å and for *c* between 6.58 and 6.75 Å; similar values were found by Kong et al. and Wang [29, 30]. The *c/a* ratio of Cu₂S films is showed in Fig. 3. The determined ratio of the films is between 1.67 and 1.73; films deposited at –600 and –585 mV with treatment under sulfur atmosphere have a lesser *c/a* ratio than the stress-free sample of 1.71 [29], this favors the existence of planar defects, due to the stacking energies of faults increase

[30]. The decrease in the *c/a* ratio as the deposition potential increases may be due to the decrease of copper in the Cu₂S crystal lattice.

3.3 Morphological analysis and composition

SEM images of Cu₂S films heat-treated in an inert atmosphere at 250 °C are shown in Fig. 4. All the treatments presented a homogeneous distribution, with diverse agglomerations composed of independent copper columns [31], covered by a layer of groups of smaller particles of approximate sizes from 20 to 30 nm.

For the deposited film at a potential of –600 mV, the particles were measured using the InTouchScope™ software. The particles have an average size of approximately 250 nm (Fig. 4a). The particles of the films deposited at –585 mV are grouped in particles of 300–400 nm (Fig. 4b). The films deposited at –570 mV (Fig. 4c) had particles like those deposited at –600 mV, likewise, their sizes are approximately 250 nm. Finally, the films deposited at –555 mV showed greater uniformity in shape, the average size is approximately 200 nm (Fig. 4d).

The conditions of the post-deposition treatment, both atmosphere and temperature, transform the morphology of the deposited films, as can be seen in the micrographs of films deposited at –555 mV (Fig. 5). In an inert atmosphere at 250 °C (Fig. 5a), the crystals have an irregular shape and a homogeneous dispersion throughout the film; the size of the crystal is between 150 and 200 nm, however, agglomerations of smaller particles can be observed on the crystals [32], this effect has also been observed in the films treated at 250 °C in a sulfur atmosphere (Fig. 5c).

On the other hand, in Fig. 5b, c, which correspond to the treatment of 350 °C in inert atmosphere and sulfur, respectively, there is a stronger compact agglomeration of the material in the films in inert atmosphere (Fig. 5b) it is feasible to observe particles of up to 450 nm as well as smaller particles of approximately 250 nm. However, the size of the crystals is smaller in the films treated in a sulfur atmosphere (Fig. 5d), particles of 250 nm and particles smaller than approximately 150 nm.

The Cu/S ratio is estimated from the EDX analysis of the deposited films, and the results obtained are presented in Fig. 6. The results show that there is a copper richness in the films deposited at potentials of –600 and –585 mV with respect to those deposited at –570 and –555 mV. This difference is caused by the proximity of the potential used to the reduction potential of pure copper, approximately to –650 mV, close to that found by Dhasade et al. [32]. Films treated at 350 °C in both atmospheres and deposited at –585 and –600 mV, have an appropriate Cu:S stoichiometric ratio of 2:1.

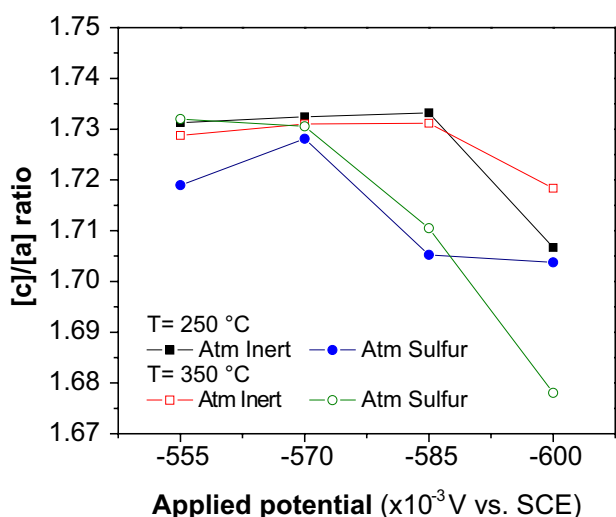


Fig. 3 Variation of [c]/[a] ratio versus applied potential of Cu₂S films deposited

Fig. 4 SEM images of Cu_2S films deposited applying a potential of **a** – 600 mV, **b** – 585 mV, **c** – 570 mV and **d** – 555 mV, heat treated at 250 °C and inert atmosphere

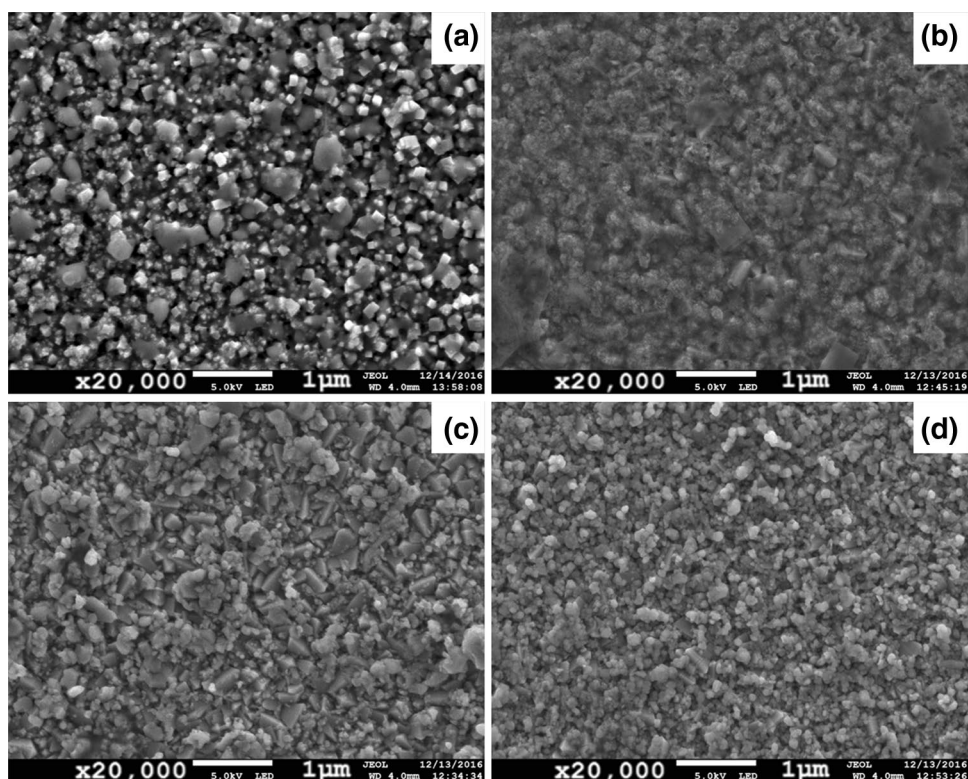
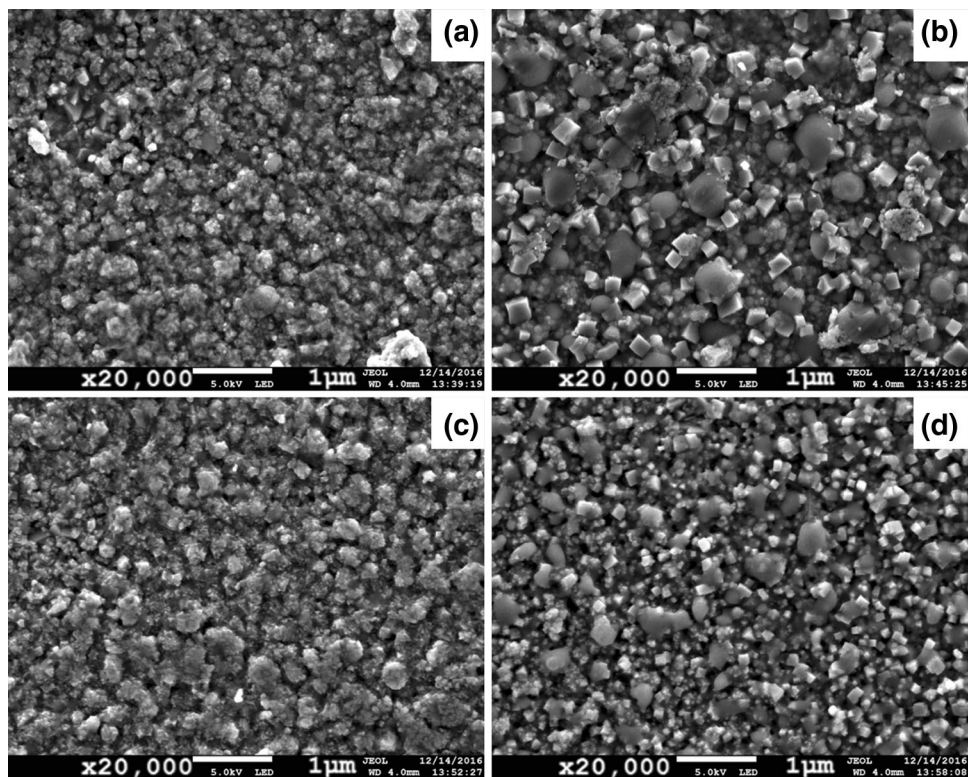


Fig. 5 SEM images of Cu_2S films deposited at –555 mV and thermally treated **a** atm. inert 250 °C, **b** atm. inert 350 °C, **c** atm. sulfur 250 °C and **d** atm. sulfur 350 °C



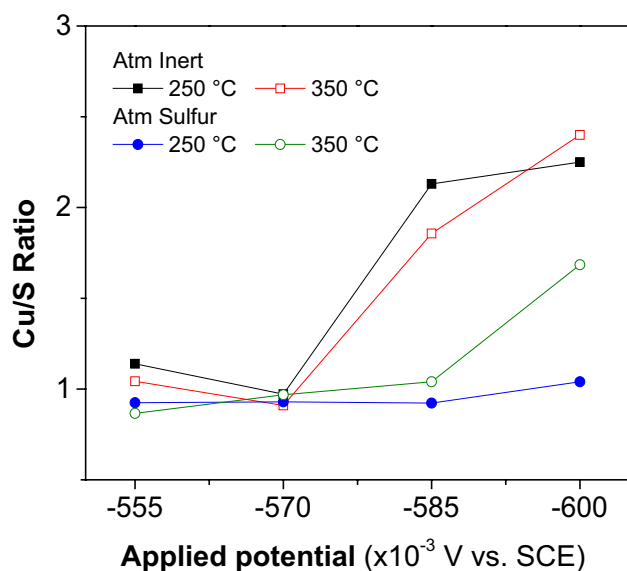


Fig. 6 Variation of the Cu/S ratio versus applied potential for the deposition of Cu_2S thin films

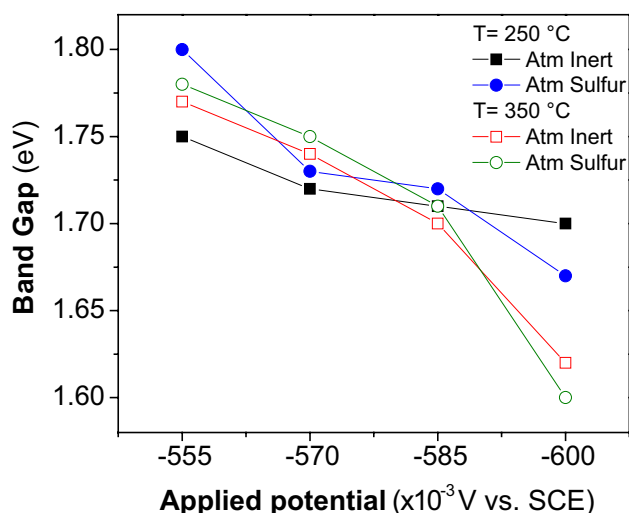


Fig. 7 Variation of band gap versus applied potential of Cu_2S thin films

3.4 Optical properties

The band gap determined by the Tauc plot $[(\alpha h\nu)^2 \text{ vs. } h\nu]$ [33] is presented in Fig. 7. In films with annealing at 250 °C, the results show that the films treated in inert atmosphere exhibit a band gap increase in the potentials of -555 and -570 mV and a decrease in -585 and -600 mV. In the films treated under sulfur atmosphere present a decrease when the applied potential decreases. This is because the presence of copper is higher in the lower potentials (-585 and -600 mV), as shown by the EDX analysis (Fig. 6). It

has been reported that the increase in the band gap is related to copper deficiency [34]. Similarly, this phenomenon occurs in films treated at 350 °C in both atmospheres. These values correspond to the indirect transition, found by Schneider et al. [35] in the range of 1.6–1.8 eV.

The results obtained in this study show that the changes in the deposition potential in electrodeposition, and in temperature and atmosphere conditions modifies the forbidden band of films. The variation of the potentials permits to modify the elemental concentration of the deposited films, in accordance with the reduction of copper and sulfur ions. The modification in the post-deposit annealing alters the crystal-line structure of the material, as well as the Cu:S ratio of the deposited films. These changes in the chemical, structural and compositional properties significantly affect the band gap. The deposit of Cu_2S films with different physical and chemical properties allows us to use this type of material in different applications, the applications can include catalysis, optoelectronics and mainly in solar cells of thin films.

4 Conclusions

Cu_2S films were deposited on FTO substrates using the electrodeposition technique. The films were deposited potentiostatically in the range of -600 to -555 mV (SCE), between the copper and sulfur reduction potentials determined by cyclic voltammetry. The crystal structure of the films is hexagonal in the chalcocite phase, and a difference in the intensity of the diffraction planes was found to be due to the presence of sulfur, caused by the proximity to the reduction potential of sulfur. The increase of sulfur was confirmed with the information obtained from the analysis of elemental composition: at the potentials at -555 and -570 mV it was found that the Cu:S ratio is lower than for deposition at -585 and -600 mV due to the lower presence of sulfur. Heat treatment causes differences in the deposition process of deposited films, in which the presence of sulfur is higher at a lower temperature, and also under sulfur atmosphere. The films deposited at -600 mV with heat treatment at 350 °C and under inert atmosphere were the best conditions, in terms of the homogeneity in morphology, the 2:1 ratio between the amount of copper and sulfur, and the approximate band gap of 1.61 eV.

Acknowledgements The authors thank M.I. Anabel González Díaz and M.C. Edith Ponce Recinos for their contribution in SEM, EDX and XRD analysis.

References

1. U. Shamraiz, A. Badshah, R.A. Hussain, M.A. Nadeem, S. Saba, J. Saudi Chem. Soc. **21**, 390 (2017)

2. Y. Ding, Y. Li, C. Liu, Z. Sun, *Solar Energy Storage* (Elsevier, New York, 2015), pp. 7–25
3. D. Li, J. Ma, L. Zhou, Y. Li, C. Zou, *Opt.—Int. J. Light Electron Opt.* **126**, 4971 (2015)
4. S. Farhadi, F. Siadatnasab, *Mater. Res. Bull.* **83**, 345 (2016)
5. S.C. Riha, R.D. Schaller, D.J. Gosztola, G.P. Wiederrecht, A.B.F. Martinson, *J. Phys. Chem. Lett.* **5**, 4055 (2014)
6. W. van der Stam, S. Gradmann, T. Altantzis, X. Ke, M. Baldus, S. Bals, C. de Mello Donega, *Chem. Mater.* **28**, 6705 (2016)
7. G. Li, M. Liu, H. Liu, *CrystEngComm* **13**, 5337 (2011)
8. M.P. Suryawanshi, S.W. Shin, U.V. Ghorpade, K.V. Gurav, C.W. Hong, P.S. Patil, A.V. Moholkar, J.H. Kim, *J. Alloys Compd.* **671**, 509 (2016)
9. J.J. Scragg, *Copper Zinc Tin Sulfide Thin Film. Photovoltaics* (Springer, Berlin, 2011), pp. 1–8
10. B. Ren, L. Wang, J. Huang, K. Tang, Y. Yang, L. Wang, *Vacuum* **112**, 70 (2015)
11. M. Venkata-Haritha, C.V.V.M. Gopi, Y.-S. Lee, H.-J. Kim, *RSC Adv.* **6**, 101185 (2016)
12. G. Mondal, S. Jana, A. Santra, M. Acharjya, P. Bera, D. Chattopadhyay, A. Mondal, P. Bera, *RSC Adv.* **5**, 52235 (2015)
13. R. Mulla, M.K. Rabinal, *Appl. Surf. Sci.* **397**, 70 (2017)
14. B. Zhang, Y. Zhang, W. Liang, X. Yu, H. Tan, G. Wang, A. Li, J. Jin, L. Huang, *RSC Adv.* **7**, 2486 (2017)
15. N.L. Botha, P.A. Ajibade, *Mater. Sci. Semicond. Process.* **43**, 149 (2016)
16. A. Cuevas, R. Romero, D. Leinen, E.A. Dalchiele, J.R. Ramos-Barrado, F. Martin, *Sol. Energy Mater. Sol. Cells* **134**, 199 (2015)
17. R. Sahraei, S. Noshadi, A. Goudarzi, *RSC Adv.* **5**, 77354 (2015)
18. X.-S. Hu, Y. Shen, L.-H. Xu, L.-M. Wang, L. Lu, Y. Zhang, *Appl. Surf. Sci.* **385**, 162 (2016)
19. U. Shamraiz, R.A. Hussain, A. Badshah, *J. Solid State Chem.* **238**, 25 (2016)
20. A. Vasuhi, R.J. Xavier, R. Chandramohan, S. Muthukumaran, K. Dhanabalan, M. Ashokkumar, P. Parameswaran, *J. Mater. Sci.: Mater. Electron.* **25**, 824 (2014)
21. W. Dang, X. Ren, W. Zi, L. Jia, S.F. Liu, *J. Alloys Compd.* **650**, 1 (2015)
22. H. Borchert, *Solar Cells Based Colloid. Nanocrystals* (Springer International Publishing, Cham, 2014), pp. 111–117
23. K. Anuar, Z. Zainal, M.Z. Hussein, H. Ismail, *J. Mater. Sci.: Mater. Electron.* **12**, 147 (2001)
24. S.G. Lee, J. Kim, H.S. Woo, Y. Jo, A.I. Inamdar, S.M. Pawar, H.S. Kim, W. Jung, H.S. Im, *Curr. Appl. Phys.* **14**, 254 (2014)
25. A. Giaccherini, S. Cinotti, A. Guerri, F. Carlà, G. Montegrossi, F. Vizza, A. Lavacchi, R. Felici, F. Di Benedetto, M. Innocenti, *Sci. Rep.* **7**, 1615 (2017)
26. S. Wang, L. Guo, X. Wen, S. Yang, J. Zhao, J. Liu, Z. Wu, *Mater. Chem. Phys.* **75**, 32 (2002)
27. A.H. Ismail, A.H. Abdullah, Y. Sulaiman, *Superlatt. Microstruct.* **103**, 171 (2017)
28. H. Borchert, *Solar Cells Based Colloid. Nanocrystals* (Springer International Publishing, Cham, 2014), pp. 79–94
29. D. Kong, A. Xu, C. Dong, F. Mao, K. Xiao, X. Li, D.D. Macdonald, *Corros. Sci.* **116**, 34 (2017)
30. L.-W. Wang, *Phys. Rev. Lett.* **108**, 85703 (2012)
31. K. Zhao, H. Yu, H. Zhang, X. Zhong, *J. Phys. Chem. C* **118**, 5683 (2014)
32. S.S. Dhasade, J.S. Patil, S.H. Han, M.C. Rath, V.J. Fulari, *Mater. Lett.* **90**, 138 (2013)
33. J. Tauc, R. Grigorovici, A. Vancu, *Phys. Status Solidi* **15**, 627 (1966)
34. P. Roy, S.K. Srivastava, *CrystEngComm* **17**, 7801 (2015)
35. N. Schneider, D. Lincot, F. Donsanti, *Thin Solid Films* **600**, 103 (2016)